Single Event Rates for Devices Sensitive to Particle Energy

L. D. Edmonds, L. Z. Scheick, *Member, IEEE,* and M. W. Banker

***Abstract*—Single event rates (SER) can include contributions from low-energy particles such that the linear energy transfer (LET) is not constant. Previous work found that the environmental description that is most relevant to the low-energy contribution to the rate is a "stopping rate per unit volume" even when the physical mechanisms for a single-event effect do not require an ion to stop in some device region. Stopping rate tables are presented for four heavy-ion environments that are commonly used to assess device suitability for space applications. A conservative rate estimate utilizing limited test data is derived, and the example of SEGR rate in a power MOSFET is presented.**

I. Introduction

SINGLE-event rate calculations for semiconductor devices that are sensitive to ion test conditions involve special considerations such as ion energy deposition at low ion energies. In particular, single-event gate rupture (SEGR) in power MOSFETs exposed to space environments can include contributions from low-energy particles in which the linear energy transfer (LET) varies significantly as the particle travels through the active region of the device. A natural space environment such as galactic cosmic rays (GCR) contains a mixture of particle energies. While most of these particles have high energies (in the sense that the LET is nearly constant within a device), these are not necessarily the dominant contribution to the SEGR rate. Earlier work by Titus, Liu, and others [1], [2], found that the worst-case (from the point of view of SEGR susceptibility) ion energy places the Bragg Peak near a selected location within the device. Hence, the worst-case energy for a given ion specie gives the ion a short range. Recent work in [3], [4], and [5] have shown similar effects on MOSFETs and SET in linear devices [6].

An SEGR rate calculation algorithm for such a situation was derived in [7], which also explained that an expected rate is a useful concept even for destructive events (such as SEGR) because this rate is an input to a Poisson probability calculation for assessing mission risk. However, the rate calculation algorithm in [7] has a major disadvantage in that a complete set of data needed for rate calculations requires that the device be tested with every ion specie at every energy. In practice, test data are limited to a few ion species at a few selected energies. One objective of this paper is to show how upper bound (i.e., conservative) SEGR rate estimates can be obtained from a limited data set. Previous work [7] found that the environmental description most relevant to the low-energy contribution to the rate is a "stopping rate per unit volume" assigned to each ion specie. This concept is relevant even when the physical mechanisms for a single-event effect do not require an ion to stop in some device region. The estimates given here utilize these stopping rates. A second objective of this paper is to construct stopping rate tables for four heavy-ion environments that are commonly used to assess device suitability for space applications.

The research in this paper was carried out at the Jet Propulsion Laboratory, California Institute of Technology, under a contract with the National Aeronautics and Space Administration. Reference herein to any specific commercial product, process, or service by trade name, manufacturer, or otherwise, does not constitute or imply its endorsement by the United States Government or the Jet Propulsion Laboratory, California Institute of Technology.

L. D. Edmonds is a private consultant (phone: 818-720-6660; e-mail: larry.d.edmonds73@gmail).

L. Z. Scheick is with the Jet Propulsion Laboratory, California Institute of Technology, Pasadena, CA 91109 USA (e-mail: leif.z.scheick@jpl.nasa.gov).

M. W. Banker is with the Dept. of Electrical Engineering, University of Florida, Gainesville, FL, USA (e-mail: Mbanker@ufl.edu).

II. Definition of the Design Case

A. The Ion Environment

We consider a design-case device exposed to a hypothetical space environment. The hypothetical environment considered here is an ordered set of ions. An "ordered set" is defined by the property that if ion LET is plotted against ion range (instead of energy) the plot will show the heavier ion as having the larger LET. Ion species found in the GCR spectrum do not form an ordered set. This is seen in Fig. 1, depicting plots of LET versus range (calculated by the 2008.04 version of the SRIM code [8]) for several example ions commonly used for single-event effects testing. The lighter ions shown in Fig. 1a almost form an ordered set, but not exactly (e.g., the LET of argon is less than the LET of the lighter silicon when the range is between 1 and 2 μm), but this discrepancy is small enough to be ignored. Larger discrepancies (e.g., nickel compared to other ions in Fig. 1d) cannot be ignored. Section IV addresses this fact with recommendations regarding test-ion selection to minimize this issue. By following these recommendations, an analysis derived for an ordered set of ions will be able to produce upper bound rate estimates in spite of the fact that a real environment is not an ordered set. Therefore, it is useful to consider the hypothetical case of an ordered set. Note that an ordered set has the property that

$$\begin{aligned} &\textit{If} \quad j \geq i \quad \textit{then} \\ &L_j(\tau, x) \geq L_i(\tau, x) \quad \textit{for all } x \textit{ and all } \tau \end{aligned} \tag{1}$$

where $L_i(\tau, x)$ is the LET at a depth x in a material from specie i (atomic number i) with incident range τ. After an ion stops, it no longer carries any energy. This is reflected in the notation used here by defining $L_i(\tau, x)$ to be zero if $x > \tau$.

B. The Design-Case Device

Loosely speaking, the design-case device is defined by the property that LET is the relevant ion parameter for determining whether a single-event effect (SEE) will occur. However, additional explanation is needed when considering short-range ions because LET varies with location on the ion track. For a more precise definition of the design-case device,

we compare two ions that hit the device at the same location and travel in the same direction. Suppose that at every (the word "every" is important) point on the track produced by the first ion, the LET of the first ion at that point is greater than or equal to the LET of the second ion at the same point (the LET is taken to be zero beyond the end of a track so that LETs can be compared at the same location even if the two ions produce different track lengths). The property that defines the design-case device is that, for any example satisfying the stated conditions, the first ion is at least as capable as the second of producing an SEE. Using notation in Section II-A, this property is written as

$$\begin{aligned}&\text{If specie } i \text{ with incident range } \tau_i \text{ produces SEE,}\\&\text{and if specie } j \text{ with incident range } \tau_j \text{ satisfies}\\&L_j(\tau_j, x) \ge L_i(\tau_i, x) \text{ at each } x \text{ in the device, then}\\&\text{specie } j \text{ with incident range } \tau_j \text{ produces SEE.}\end{aligned} \tag{2}$$

III. Upper Bound Rates for the Design case

This work is a continuation of [7] which separated the particle environment into a high-energy group and a low-energy group. This separation is defined by the user by selecting an ion range, called the "demarcation range," denoted τ_D. Ions, regardless of specie, having ranges less than τ_D are classified as short-range (a.k.a., low-energy) ions, and ions having ranges greater than τ_D are classified as long-range (a.k.a., high-energy) ions. There is some flexibility (discussed later) in the choice of a demarcation range but the choice is not completely arbitrary because different approximations are used for the two groups of ions. For a tentative choice to be usable, it must satisfy the simultaneous conditions of being both "small enough" and "large enough." It is "small enough" when an approximation used in [7] to estimate the low-energy flux inside a spacecraft is valid. It was found in [7] that if the spacecraft shielding consists of at least 100 mils of aluminum, the demarcation range is small enough if it does not exceed 500 μm in silicon. The demarcation range is "large enough" when ions having a greater range can be approximated as having a nearly uniform LET as the ion travels through the device active region. A range that satisfies this condition depends on the device considered (an example is given in Section VI) but, in general, as long as the dimensions of the device active region are very much smaller than the spacecraft shield thickness (assumed to be the case), there will exist a demarcation range that is both short enough and long enough.

Estimates of single-event rates in space typically assume a nearly isotropic ion environment and that assumption is used here. The low-energy contribution, denoted here as SER_{low}, was calculated in [7] via

$$SER_{low} = \sum_i s_i \int_0^{\tau_D} \overline{\chi}_i(\tau)\ d\tau$$

where the sum includes the atomic numbers of all heavy-ions in the environment, s_i is the stopping rate per unit volume for ion specie i (a characteristic of the environment) as defined in [7] (and discussed again in Section V), and $\overline{\chi}_i(\tau)$ is the directional-average single-event cross section for specie i when the incident energy produces a range τ in the device active region. The high-energy contribution, denoted SER_{hi}, includes only those ions having a range greater than τ_D. These ions have a nearly uniform LET in the device active region. We assume that such ions are adequately described by specifying LET alone, so a modification (to omit low-energy particles) of [9, Eq.(10)] gives

$$SER_{hi} = \int_0^{\infty} h(\tau_D, L)\, \overline{\sigma}(L)\, dL$$

where $\overline{\sigma}(L)$ is the directional-average single-event cross section for long-range (constant-LET) ions having LET L, and $h(\tau_D,L)$ is the differential (in LET) omnidirectional particle flux as a function of LET and evaluated at the part location. The argument τ_D indicates that the flux $h(\tau_D,L)$ is to include only those ions having ranges greater than τ_D. The total rate, denoted SER, is given by

$$SER = \sum_i s_i \int_0^{\tau_D} \overline{\chi}_i(\tau)\ d\tau + \int_0^{\infty} h(\tau_D, L)\, \overline{\sigma}(L)\, dL\,. \tag{3}$$

The first term on the right side of (3) is the low-energy contribution to the rate, and the second term is the high-energy contribution.

An unfortunate property of (3) is that it requires information that is unlikely to be known from test data because the sum on the right includes every specie of heavy ion in the environment. To obtain conservative rate estimates from limited test data, let N denote the number of species used for the test. Let I_1 denote the atomic number of the lightest test ion. I_2 is the atomic number of the second lightest test ion, etc., so I_N is the atomic number of the heaviest test ion. This assigns values to each of the numbers, I_1, I_2, …, I_N. An ion bin is a set of numbers. The first bin, denoted B_1, is the set of atomic numbers i satisfying $2 \le i \le I_1$.[1] The second bin, denoted B_2, is the set of atomic numbers i satisfying $I_1 < i \le I_2$, etc. Given that a design-case device, which satisfies (2), is exposed to an ordered set of ions, which satisfies (1), we can use (1) and (2) to conclude that

$$\begin{aligned}&\textit{If} \quad j \ge i \quad \textit{then}\\&\int_0^{\tau_D} \overline{\chi}_j(\tau)\ d\tau \ge \int_0^{\tau_D} \overline{\chi}_i(\tau)\ d\tau\,.\end{aligned}$$

A particular application of this inequality is

$$\sum_{i \in Bn} s_i \int_0^{\tau_D} \overline{\chi}_i(\tau)\ d\tau \le \left(\sum_{i \in Bn} s_i \right) \int_0^{\tau_D} \overline{\chi}_{In}(\tau)\ d\tau \tag{4a}$$

for each $n = 1,\ldots,N$. In the notation here, the label $i \in B_n$ below a sum means to sum over those values of i that are contained in the bin B_n. To obtain bounds for ions heavier than the heaviest test ion, it is necessary to find some upper bound for the cross section (e.g., from the geometric area of

[1] Protons require a separate treatment not given in this paper because their effects are often caused by indirect ionization instead of direct ionization. This paper considers only effects caused by direct ionization, so the smallest i considered here is 2.

some device structure) denoted $\overline{\chi}_{UB}$ and satisfying $\overline{\chi}_i(\tau) \le \overline{\chi}_{UB}$ so that

$$\sum_{i>I_N} s_i \int_0^{\tau_D} \overline{\chi}_i(\tau)\ d\tau \le \left(\sum_{i>I_N} s_i \right) \overline{\chi}_{UB}\ \tau_D . \tag{4b}$$

Combining (4) with (3) gives

$$SER \le \sum_{n=1}^{N} \left(\sum_{i \in Bn} s_i \right) \int_0^{\tau_D} \overline{\chi}_{In}(\tau)\ d\tau + \left(\sum_{i>I_N} s_i \right) \overline{\chi}_{UB}\ \tau_D + \int_0^{\infty} h(\tau_D, L)\, \overline{\sigma}(L)\, dL \tag{5}$$

It was previously stated that there is some flexibility in the selection of the demarcation range τ_D. Using terminology in [7], there is an "overlap" interval such that any range selected from this interval is both small enough and large enough to qualify as a demarcation range (i.e., the approximations used for the low-energy calculations, and the approximations used for the high-energy calculations, are both accurate). Replacing one selection of the demarcation range with a different selection within this overlap interval will cause some ions to be moved out of one of the two groups (low-energy or high-energy) and into the other group, but these ions will still be accurately represented. Therefore, when using (3) to calculate the rate (which requires unlimited test data), different allowed choices of the demarcation range will affect the low-energy and high-energy contributions individually, but the total calculated rate will be nearly the same for any allowed choice of a demarcation range. However, there is a greater distinction between different choices of demarcation range when using (5) to calculate an upper bound for the rate. The reason is that the inequalities in (4) produce some conservatism in the calculated low-energy contribution that is not also present in the high-energy contribution, so there may be some motivation (to reduce conservatism) in selecting the smallest range that qualifies as a demarcation range. In practice, the most convenient demarcation range depends on the available test data.

We now specialize to the case of SEGR. That a device is a design-case device as defined in Section II-B was already assumed when deriving (5), but we will now simplify (5) for the special case of SEGR. We follow recommendations in [10], which state two device properties that are expected to be adequate approximations for describing SEGR in a real device. The first property states that the normal-incident cross section is approximately a step function. For any ion specie, ion energy, and biasing voltage for which the device is susceptible to SEGR, the normal-incident cross section is some constant denoted A (which [10] calls the "SEGR sensitive area"). For all other species, energy, and voltage combinations, the normal-incident cross section is zero. The second property is concerned with directional effects. Unlike some other types of single-event effects in which the cosine law is sometimes an adequate approximation, a better approximation for SEGR utilizes an angular cutoff [10]. Following [10], the directional cross section for an arbitrary direction is taken to be the normal-incident cross section if the direction lies in a solid angle that is a characteristic of the device, and the directional cross section is zero for trajectories outside this solid angle. The result is that the directional-average cross section for an ion able to produce SEGR at normal incidence is fA, where f is the fractional solid angle of susceptibility (a device characteristic and is the solid angle of susceptibility divided by 4π steradians). These assumptions give

$$\int_0^{\infty} h(\tau_D, L)\, \overline{\sigma}(L)\, dL = fA\, H(\tau_D, L_{th}) \tag{6a}$$

$$\overline{\chi}_{UB} = fA \tag{6b}$$

$$\int_0^{\tau_D} \overline{\chi}_i(\tau)\ d\tau = fA \Delta_i \tau \tag{6c}$$

where L_{th} is the threshold LET for high-energy ions, H is the integral (in LET) flux, and $\Delta_i\tau$ is the width of the portion of the interval $[0,\tau_D]$ satisfying $\overline{\chi}_i(\tau) > 0$ (an algorithm for calculating $\Delta_i\tau$ is explained in Section VI). Substituting (6) into (5) gives

$$SER \le fA \sum_{n=1}^{N} \left(\sum_{i \in Bn} s_i \right) \Delta_{In}\tau + fA \left(\sum_{i>I_N} s_i \right) \tau_D + fA\, H(\tau_D, L_{th}) \tag{7}$$

IV. Practical Issues for a Real Case

The design-case device described in Section II-B is expected to be an adequate representation of a real device, but real ions do not produce an ordered set. For example, the LET of nickel is much less than the LET of many of the lighter ions when the range is only a few microns, as seen in Fig. 1d. If a rate calculation uses nickel test data to estimate single-event responses from other ions, the prediction tends to be optimistic. To obtain conservative rate estimates, it is recommended that nickel not be used as a test ion for the low-energy tests. Another specie that might be excluded from low-energy tests is gold, but this is a marginal case so a recommendation regarding the suitability of gold is not given here. All other species represented in Fig. 1 are suitable for low-energy tests for the purpose of obtaining conservative rate estimates using the calculation method derived here because violations of the ordered set property (where there are violations) are small enough to ignore. Test ions should include iron because this is the most abundant of the very heavy ions in space.

V. Stopping Rates for Example Environments

Four examples given here include two spacecraft shield thicknesses (100 and 250 mils of aluminum) in two environments (GCR in interplanetary space during solar minimum and a solar flare in interplanetary space at 1AU). These shield thicknesses were selected because 100 mils of aluminum is the default assumption used by radiation specialists when no other information is given, whereas 250 mils is a more realistic amount of shielding likely to be found

on a spacecraft when all spacecraft structures are included. The solar flare environment is, more specifically, the "worst-week flare" (WWF) used in the familiar CREME96 code. It is useful because a worst-week SER multiplied by 7.5 days is an estimate of the number of SEEs expected to be accumulated over the duration of the model flare, which is relevant to risk estimates.

Calculating the stopping rate per unit volume of each ion in silicon using the method in [7] is a multi-step process requiring the use of two different software programs, the Stopping and Range of Ions in Matter (SRIM) and CREME-MC,[2] both available from the Internet. The first step is to use SRIM to calculate the energy for each ion just able to penetrate the spacecraft shielding. This energy is denoted $E_{T,i}$, where i is the atomic number of the element being used, and T is the shield thickness. The energy for the desired amount of shielding is found by interpolating a range-energy table produced by SRIM. For example, energies for 2.48 mm and 2.73 mm may be given by SRIM, but the energy for 2.54 mm (100 mils) must be interpolated (a linear interpolation was used here). Then, SRIM is used again to calculate the LET, denoted $L_i(E_{T,i})$, in the target material (silicon for the results given here) for the energy of the ion found in the first step. Once again, an interpolation will be needed.

The stopping rate for a given particle specie is calculated from a differential flux for that specie evaluated outside the spacecraft shielding. The CRÈME-MC program is used for this calculation. This program uses energy per nucleon instead of total energy to describe a heavy ion, so an input given to the code is obtained by dividing $E_{T,i}$ calculated above by the atomic mass unit (amu) for the particular ion to get $E_{T,i}/m$, measured in eV/nucleon or MeV/nucleon. Then, use CRÈME-MC to find the differential flux evaluated at this energy outside the spacecraft shielding. This flux is denoted $h^*(E_{T,i}/m)$ (not to be confused with the flux in Section III that is a function of LET). This is a directional flux that is differential in energy-per-nucleon, and the units are particles/m^2-s-sr-MeV/nucleon. However, the flux used to calculate the stopping rate is omnidirectional (no steradians in the units) and differential in energy (instead of energy per nucleon) and has the units of particles/cm^2-day-MeV. The latter flux is denoted $h_{U,OMNI}(E_{T,i})$ and it is calculated from the code output using $h_{U,OMNI}(E_{T,i}) = 108.6 \times h^*(E_{T,i}/m)/m$. Finally, the stopping rate per unit volume for the ion is calculated by $s_i = \rho\, L_i(E_{T,i}) \times h_{U,OMNI}(E_{T,i})$, where ρ is the density of silicon, 2.33 g/cm^3 = 2.33×10^3 mg/cm^3. The units for the stopping rate per unit volume are particles/cm^3-day.

An excerpt from a spreadsheet showing all calculations for a few examples is shown as Fig. A in the Appendix. Table A in the Appendix lists the final results for all ions in each of the four environments. In this table, the columns labeled "Z" contain the atomic numbers and all other columns contain the stopping rates per unit volume in the units of 1/cm^3-day. These are the environmental parameters (as opposed to device parameters) used in (3) to predict the response of a device to an environment. Each environmental parameter has a literal physical interpretation as the rate that an ion specie stops in a small volume (which motivated the name "stopping rate per unit volume") as explained in [7]. These environmental parameters can have a variety of applications so protons were included in Table A even though they are not relevant (because they do not contribute via direct ionization) to the type of device response considered in this paper.

[2] CREME-MC replaced CREME96 as the publicly-available code but options available in CREME-MC include the same models and algorithms originally in CREME96, which are the models and algorithms used for this work.

VI. SEGR Rate Method with an Example

A step-by-step method for obtaining conservative (upper bound) estimates of SEGR rates in space is given. An example is included for illustration.

Step 1: Obtain Heavy-Ion Data

Select a device of interest, a Vgs biasing condition of interest, and follow the customary procedure for obtaining heavy-ion SEGR data. This procedure starts with a selected ion specie and incident energy and increases Vds in steps until an SEGR is produced. The largest Vds prior to an SEGR will be called the "last-pass voltage", and the smallest Vds that produces an SEGR will be called the "first-fail voltage." The process is repeated for other incident energies and ion species. In order for test data to be usable for the rate calculation given here, the incident energy, for each ion specie, must vary from very small to very large. "Very small" means that the Bragg Peak is in the proximity of the silicon surface of incidence. "Very large" means that the LET is nearly constant in the device active region. Recommended species for these tests include lithium, carbon, oxygen, fluorine, neon, silicon, phosphorus, chlorine, argon, iron, arsenic, bromine, krypton, silver, iodine, and xenon. As mentioned earlier in context with Fig. 1d, nickel is not recommended for low-energy tests. Gold is a marginal case. It might actually be useable, but excluding it when it is usable is an error on the side of caution.

An example of such a data set is shown in Table I which was taken from [11]. The device is not identified due to proprietary issues. All tests that produced Table I were done at Vgs = 0. The maximum Vds rated by the manufacturer is 100 V. Any entry in Table I indicating that Vds is greater than some value is interpreted to mean that this value is the largest voltage that was tested and no SEGR was observed at this voltage. All other entries in the table are midway between the last-pass voltage and first-fail voltage (the Vds increments were 10 V, so the last-pass voltage is 5 V less than the table entry, and the first-fail voltage is 5 V greater than the table entry). The device has an epi thickness of 17.8 μm [11]. Note that one of the test ions is gold, but a later discussion (under Step 5) will explain why this is not an issue for the rate calculation given as an example here. It is unfortunate, as seen later, that the test ions did not include iron.

Step 2: Select a Demarcation Range

The demarcation range was explained in Section III. For the example data set in Table I, it is convenient to use 200 μm as the demarcation range, but we must verify that 200 μm qualifies. The spacecraft shielding in the example below will

be 100 mils of aluminum, so as noted in Section III, 200 μm is small enough to qualify. The only question that remains is whether the LET, of ions having this range when entering the device active region, is nearly constant as the ion travels through the active region. We assume that the thickness of the active region is roughly equal to the epi thickness (about 20 μm). Consider an ion that has an initial (when entering the active region) range of 200 μm, so it exits this 20 μm region with a range of 180 μm. The data represented in Fig. 1 show that the variation in LET, for any ion specie included in the figure, is only about 5% between entering and exiting the active region. This is considered here to be a nearly constant LET, so 200 μm is allowed as a demarcation range, and that is the demarcation range that will be used in the example given here.

Step 3: Construct Ion Bins

The ion bins were explained in the paragraph just below (3). For the example in Table I, the lightest test ion is argon (I_1 = 18), the second lightest is krypton (I_2 = 36), the second heaviest is xenon (I_3 = 54), and the heaviest is gold (I_4 = 79). Therefore, the bin B_1 contains the numbers from 2 to 18, the bin B_2 contains the numbers from 19 to 36, the bin B_3 contains the numbers from 37 to 54, and the bin B_4 contains the numbers from 55 to 79. For this example, (7) becomes

$$SER \le fA\left\{\Delta_{18}\tau\sum_{i=2}^{18}s_i + \Delta_{36}\tau\sum_{i=19}^{36}s_i + \Delta_{54}\tau\sum_{i=37}^{54}s_i + \Delta_{79}\tau\sum_{i=55}^{79}s_i + \tau_D\sum_{i=80}^{92}s_i + H(\tau_D, L_{th})\right\} \quad \text{(example)}. \tag{8}$$

Step 4: Select an Environment and Sum Stopping Rates

The stopping rate per unit volume is denoted s_i for specie i and depends on the environment considered. After selecting an environment so that the stopping rates are determined, the stopping rates are summed over ion bins.

For the example considered here, the sums over bins are the sums in (8). The environment selected for this example consists of galactic cosmic rays in interplanetary space during solar minimum conditions, with spacecraft shielding of 100 mils of aluminum. The stopping rates per unit volume for this environment are included in Table A in the Appendix and summing these rates gives

$$\begin{aligned}
&\sum_{i=2}^{18}s_i = 1.74\times10^{3}\ /\text{cm}^3\text{ - day}\\
&\sum_{i=19}^{36}s_i = 2.41\times10^{1}\ /\text{cm}^3\text{ - day}\\
&\sum_{i=37}^{54}s_i = 1.75\times10^{-3}\ /\text{cm}^3\text{ - day} \qquad \text{(example)}.\\
&\sum_{i=55}^{79}s_i = 6.45\times10^{-4}\ /\text{cm}^3\text{ - day}\\
&\sum_{i=80}^{92}s_i = 5.53\times10^{-5}\ /\text{cm}^3\text{ - day}
\end{aligned} \tag{9}$$

Step 5: Select a Vds of Interest and Construct Δτ

The goal is to calculate each $\Delta\tau$ that appears on the right side of (8). These quantities depend on the ion specie and also on the value of Vds that the device will be operating at. After selecting a specie and a Vds, there are three possibilities. For the first possibility, called Case-1, the device is immune to this specie at the given operating voltage for any ion range up to the demarcation range. For this case we use $\Delta\tau$ = 0. The remaining two possibilities subdivide of the case in which there exists an incident energy at which the selected specie will produce an SEGR at the selected operating voltage. We therefore now assume there is an incident energy at which an SEGR will occur. In general, there will be an upper limit for the ion range, denoted τ_b, and a lower limit for the ion range, denoted τ_a, having the property that an SEGR will occur if and only if the ion range is between these limits. The lower limit τ_a will be less than the demarcation range, but the upper limit τ_b could be much greater than the device dimensions. This will be true if very large incident energy is needed to reduce the LET enough to make the ion incapable of producing an SEGR. One possibility, called Case-2, is that τ_b is less than the demarcation range τ_D. For this case, we use $\Delta\tau = \tau_b - \tau_a$. The last possibility, called Case-3, is that τ_b is greater than or equal to τ_D. For this case, we use $\Delta\tau = \tau_D - \tau_a$.

For the example given here, Vds is arbitrarily taken to be 80 V. It is seen from Table I that, at this voltage, the device is immune to argon for ranges up to 200 μm. This example belongs to Case-1 discussed above and the result is

$$\Delta_{18}\tau = 0 \quad \text{(example)}. \tag{10a}$$

Now consider the krypton data in Table I. Here we need a little more resolution by recognizing the distinction between the last-pass voltage (5 V less than a table entry) and the first-fail voltage (5 V greater than a table entry). The true threshold voltage for a given ion range is somewhere between the last-pass and first-fail. A conservative assumption is that the true threshold voltage is very close to the last-pass voltage, so we subtract 5 V from the table entries and conclude that krypton will produce an SEGR at 80 V when the range is between 25 and 60 μm. This example belongs to Case-2 discussed above.

The experimental data were not sufficiently complete to find the lower limit for the range, so we will conservatively take the lower limit to be zero. The result is

$$\Delta_{36}\tau = 60 - 0 = 60\ \mu\text{m} \quad \text{(example)}. \tag{10b}$$

Finally, consider the xenon and gold data in Table I. At an operating voltage of 80 V, the data show the upper limit for the range is greater than 200 μm, which is the demarcation range, so each of these examples belong to Case-3 discussed above. The experimental data were not sufficiently complete to find the lower limit for the range, so we will conservatively take the lower limit to be zero. The result is

$$\Delta_{54}\tau = 200 - 0 = 200\ \mu\text{m} \quad \text{(example)} \tag{10c}$$

$$\Delta_{79}\tau = 200 - 0 = 200\ \mu\text{m} \quad \text{(example)}. \tag{10d}$$

Note that (10d) is the maximum value that can be assigned to $\Delta\tau$, which explains why gold is a suitable test ion for this example. Substituting (9) and (10) into (8) gives

$$SER \le fA\left\{\frac{0.1446}{\text{cm}^2\text{ - day}} + H(\tau_D, L_{th})\right\} \quad \text{(example)}. \tag{11}$$

The first term in the curly bracket in (11) is a conservative estimate of the low-energy contribution, and the second term (not yet numerically evaluated) is the high-energy contribution. In this example, about half of the first term is from iron, and nearly all of the remainder of the first term is divided among atomic numbers that are close to that of iron.

Step 6: Estimate the High-Energy Threshold LET

The goal is to estimate L_{th} applicable to high-energy (constant-LET) ions. The general technique can be explained by an illustration. The high-energy (200-μm range) entries in Table I are shown separately in Table II. The example operating voltage considered is 80 V, and the goal is to use Table II data to find the LET corresponding to this voltage. The data in Table II are too coarse, in this example, for an empirical curve fit (with LET plotted against Vds) to be convincing. Instead, we use a conservative estimate of the LET by setting it equal to the incident LET of the heaviest test ion that did not produce an SEGR at 80 V. In this example we have L_{th} = 23.6 MeV-cm^2/mg.

Step 7: Estimate the High-Energy Flux

The goal is to estimate $H(\tau_D,L_{th})$. CREME96 calculations use three steps. The first step constructs flux versus energy spectra outside the spacecraft for a selected environment. For the example considered here, the selected environment is GCR outside the magnetosphere during solar minimum conditions. The second step transports these spectra through the spacecraft shielding (100 mils of aluminum for the example given here). Both of these steps include all ion species contained in the CREME96 model (atomic numbers 1 through 92, but it is not essential that protons be included because SEE by indirect ionization is not considered here), and default values are used for all inputs not explicitly stated above. The third step converts the flux versus energy spectra into a flux versus LET spectrum. This is the step where we omit low-energy particles from the flux. The goal is to eliminate all ions having ranges less than τ_D (200 μm for the example considered here). CREME96 allows the user to eliminate all ions having energy per mass (E/m) less than a specified value, but, unfortunately, the E/m that produces a range of 200 μm is different for different ion species. A cumbersome but generally applicable approach is to divide the set of ion species into user-selected groups (CREME96 allows the user to specify the atomic numbers to be included in the LET flux) selected so that different ions in the same group have nearly the same E/m, apply the appropriate cutoff when calculating the flux for each group, and then sum the fluxes.

A simpler approach can be used for the example considered here because, for this example, the calculated SEGR rate is almost entirely from iron and from ions having atomic numbers close to that of iron. Therefore, a single value of E/m, calculated for iron, can be applied to the entire set of ions. The range of iron in silicon is 200 μm when the energy is about 900 MeV, or E/m is about 16 MeV/nuc. Calculating the LET flux using this cutoff, evaluating the flux at an LET of 23.6 MeV-cm^2/mg (or 23600 MeV-cm^2/g), and multiplying the flux by 108.6 to convert a directional flux in CREME96 units into an omnidirectional flux in the units of 1/cm^2-day, gives

$$H(\tau_D, L_{th}) = \frac{1.5\times10^{-4}}{\text{cm}^2\text{ - day}} \quad \text{(example)}. \tag{12}$$

This is considered negligible compared to the low-energy contribution, the first term in the curly bracket in (11). The reason that these two numbers are so different can be understood by considering iron, which is the most abundant of the very-heavy ions. The maximum LET of iron in silicon is about 29 MeV-cm^2/mg, so there are some iron ions with an LET greater than 23.6. However, all such ions have a range less than 200 μm, so there are no iron ions having an LET greater than 23.6 and also having a range greater than 200 μm. Therefore, the high-energy flux H contains no iron ions at all (in fact, iron ions with LET greater than 14 have ranges less than 200 μm and are therefore classified here as low-energy ions). In contrast, the calculated low-energy contribution does include a subset of the iron population so this is the dominant contribution.

Step 8: Estimate *fA* and Calculate the Rate

We have no information about f, so we use a conservative value of 1. For this example, the die area is 1 cm^2, so we use fA = 10^{-3} cm^2, which has been typically seen in the literature. Substituting this into (11), with H neglected because of (12), a conservative estimate of the SER is 0.00013/day, so the mean time to the first SEGR is conservatively estimated to be roughly 20 years.

VII. Comparison with a more Traditional Estimate

A more traditional estimate of the SEGR rate does not separate ions into a low-energy group and a high-energy group. Instead, all ions are treated as if they have a constant LET in the active region. The relevant flux in space is then the flux of all ions, regardless of range,[3] having an incident LET that exceeds the device threshold LET (we assume here that high-energy test ions were used to find the threshold LET). Using the notation in (7), the estimated rate is the quantity $fAH(0,L_{th})$. There are two errors in this rate estimate. The first error includes ions that should have been excluded. These are ions that enter the active region with an incident LET greater than L_{th}, but have ranges short enough so that the average LET in the active region is too small to produce an SEGR. The other error excludes ions that should have been included. These are ions that enter the active region with an incident LET less than L_{th}, having ranges short enough so that the LET is not constant in the active region, while the ranges are also long enough so that the average LET in the active region is significantly larger than the incident LET. However, it is still interesting to compare numbers. Inputs used in Section VI were $fA = 10^{-3}$ cm^2 and $L_{th} = 23.6$ MeV-cm^2/mg. Using the same inputs to evaluate the quantity $fAH(0,L_{th})$ gives an estimated rate in the GCR environment of 0.00006/day. This is about half as large as the estimate given in Section VI, but the ratio of the two estimates will be different for different examples.

VIII. Recommendations

The steps listed in Section VI are consistently conservative. Specifically, any ion parameter that was not measured was estimated from the corresponding parameter for the next heavier ion for which a measurement was made. Another investigator might not want this level of conservatism. For example, another investigator might estimate the high-energy threshold LET from an empirical curve fit to data instead of selecting a value that is known to be too small. We do not claim that the conservative approach used here is the approach that must be used. We only claim that, if this approach is used, then the true SEGR rate can be expected to be smaller than the calculated rate. However, there is a concern that the conservatism can sometimes be excessive. For the example in Section VI, the calculated low-energy contribution to the SEGR rate includes iron (atomic number 26), which is the most abundant of the very heavy ions in space, but we have no device data for iron. Instead, krypton (atomic number 36) data were used to represent all atomic numbers from 19 to 36. It is possible that the device is immune to iron at the example voltage considered in Section VI, but we have no way of knowing this from the available data. If it is immune to iron, the rate estimate in Section VI is excessively conservative. A recommendation is that, for any example in which susceptibility to iron is thought to be a possibility, the device be tested with iron.

[3] To be technically correct, CREME96 has a default E/m cutoff of 0.1 MeV/nuc, but this is small enough so that the flux need not be distinguished (when spacecraft shielding is at least 100 mils Al) from a flux that places no restrictions on ion range.

IX. Discussion and Conclusion

The SEE rate can be calculated for devices whose SEE response is sensitive to ion range. The rate pivots on the sensitivity of the device to iron as it is relatively abundant and high in LET. When testing devices that are sensitive to ion range, test ions should include ions that have the LET and range properties of iron to minimize conservatism in the calculated rate. Of course, a larger number of test points at various ions and ion conditions will also reduce uncertainty in the SER, but the priority should be given to the sensitivity to iron or slightly heavier ions, excluding nickel. Also, the SEE cross section of the device has a direct effect on the SER. In most examples in the literature, the SEGR cross section can be approximated by a step function, and this is assumed for this work. Cross sections should be measured for more precise rate estimates.

The example given in this work only considered SEGR since it requires essentially normal-incidence ions for the effect to be seen. The theory that expresses rates in terms of a directional-average cross section is more general, but in order to apply this theory to other SEE phenomenon, it is necessary to convolve angular effects to obtain the directional-average cross section. This is a topic for future work.

The target readers are individuals responsible for before-the-fact (i.e., before a spacecraft launches) single-event rate estimates for flight projects. These individuals have a different perspective regarding rate calculations than some other individuals (e.g., those that merely compare calculated rates to prior flight observations) because of the serious consequences of a mission failure. Rate estimates are more difficult and complex for the target readers for two reasons. First, methods or models used by the target readers must be defendable in some way (at least logically convincing if no empirical assessment is available), while some other individuals are willing to use methods that are less defendable (an example is a whimsical choice for an RPP thickness when using CREME96 for a soft-error rate calculation). The second reason is related to uncertainties associated with insufficient device data. Available device data are sometimes incomplete (for example, there are no data for atomic numbers between 18 and 36 for the example in Section VI) and cost constraints might not allow additional testing. Some individuals might use credible guesses where data are missing. While this might produce a correct prediction, there is not a great deal of confidence that it will produce a correct prediction. In contrast, a target reader is more likely to use conservatism (i.e., worst-case assumptions) to compensate for uncertainties. This is unlikely to produce a correct prediction, but there is a great deal of confidence that the actual rate will not be larger than the prediction. The target readers use methods that are defendable and use conservatism to compensate for uncertainty, and the goal of this work is to provide such a method for SEGR rate estimates.

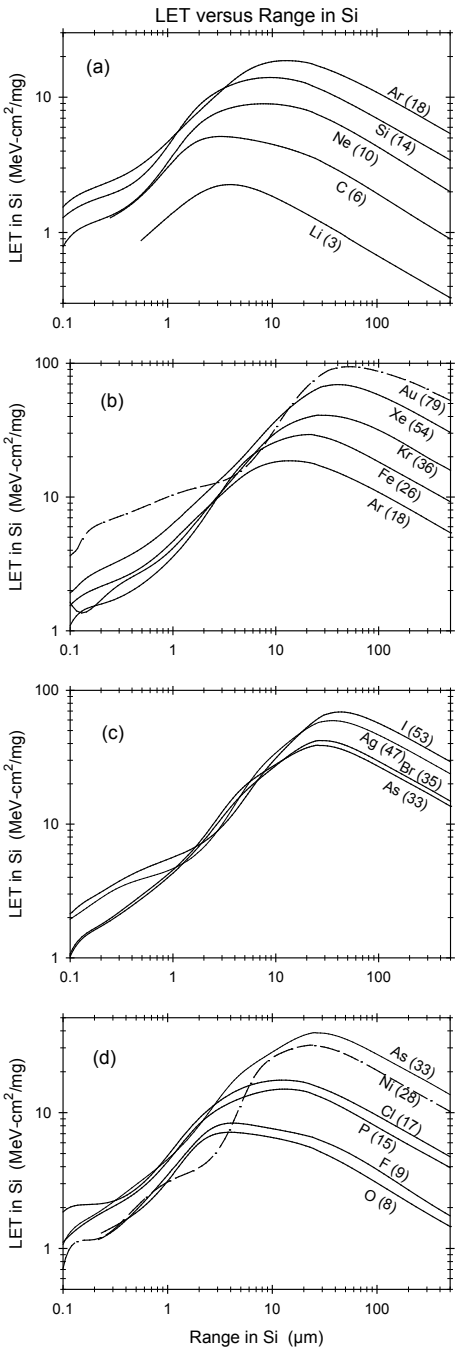

Fig. 1: A comparison between the LETs of selected ions having the same range in silicon.

REFERENCES

[1] J. L. Titus, and C. F. Wheatley, "SEE characterization of vertical DMOSFETs: An updated test protocol," *IEEE Trans. Nucl. Sci.,* vol. 50, no. 6, pp. 2341-2351, Dec. 2003.

[2] S. Liu, J. L. Titus, M. Zafrani, H. Cao, D. Carrier, and P. Sherman, "Worst-case test conditions of SEGR for power DMOSFETs," *IEEE Trans. Nucl. Sci.*, vol. 57, no. 1, pp. 279-287, Feb. 2010.

[3] V. Ferlet-Cavrois, F. Sturesson, A. Zadeh, G. Santin, P. Truscott, C. Poivey, J. R. Schwank, D. Peyre, C. Binois, T. Beutier, A. Luu, M. Poizat, G. Chaumont, R. Harboe-Sorensen, F. Bezerra, and R. Ecoffet, "Charge collection in power MOSFETs for SEB characterization—Evidence of energy effects," *IEEE Trans. Nucl. Sci.*, vol. 57, no. 6 , pp. 3515-3527, Dec. 2010.

[4] S. Liu, J.-M. Lauenstein, V. Ferlet-Cavrois, R. Marec, F. Hernandez, L. Scheick, F. Bezerra, M. Muschitiello, C. Poivey, N. Sukhaseum, L. Coquelet, H. Cao, D. Carrier, M. A. Brisebois, R. Mangeret, R. Ecoffet, K. Label, M. Zafrani, and P. Sherman, "Effects of ion species on SEB failure voltage of power DMOSFET," *IEEE Trans. Nucl. Sci.*, vol. 58, no. 6, pp. 2991-2997, Dec. 2011.

[5] J.-M. Lauenstein, N. Goldsman, S. Liu, J. L. Titus, R.L. Ladbury, H. S. Kim, A. M. Phan, K. A. LaBel, M. Zafrani, and P. Sherman, "Effects of ion atomic number on single-event gate rupture (SEGR) susceptibility of power MOSFETs," *IEEE Trans. Nucl. Sci.*, vol. 58, no. 6, pp. 2628-2636, Dec. 2011.

[6] K. Kruckmeyer, S. P. Buchner, and S. DasGupta, "Single event transient (SET) response of National Semiconductor's ELDRS-free LM139 quad comparator," *IEEE 2009 Radiation Effects Data Workshop*, pp. 65-70, 2009.

[7] L. D. Edmonds and L. Z. Scheick, "Effect of shielding on single-event rates in devices that are sensitive to particle range," *IEEE Trans. Nucl. Sci*., vol. 57, no. 6, pp. 3560-3569, Dec. 2010.

[8] Available on the Internet at: www.srim.org/

[9] L. D. Edmonds, "A method for correcting cosine-law errors in SEU test data," *IEEE Trans. Nucl. Sci.*, vol. 49, no. 3, pp. 1522-1538, June 2002.

[10] J. L. Titus, C. F. Wheatley, T. H. Wheatley, W. A. Levinson, D. I. Burton, J. L. Barth, R. A. Reed, K. A. LaBel, J. W. Howard, and K. M. VanTyne, "Prediction of early lethal SEGR failures of VDMOSFETs for commercial space systems," *IEEE Trans. Nucl. Sci.*, vol. 46, no. 6, pp. 1640-1651, Dec. 1999.

[11] N. Chatry, N. Sukhaseum, M. Sauvagnac, F. Bezerra, R. Ecoffet and R. Gaillard, "P-channel Power MOSFET SEGR sensitivity to Heavy Ion Range," Presented at the Radiation Effects on Components and Systems Conference (RADECS), 2010.

TABLE I: SEGR DATA FROM [11] FOR AN EXAMPLE 100V DEVICE

Ion	Incident Energy (MeV)	Incident LET (MeV-cm^2/mg)	Range (μm)	Vds (V)		Ion	Incident Energy (MeV)	Incident LET (MeV-cm^2/mg)	Range (μm)	Vds (V)
Ar	95	17.4	25	>100		Xe	500	69.3	40	45
Ar	115	16.6	30	>100		Xe	650	68.3	50	35
Ar	150	15	40	>100		Xe	800	66.4	60	35
Ar	185	14.1	50	>100		Xe	1100	61.9	80	35
Ar	220	13.2	60	>100		Xe	1250	59.6	90	45
Ar	245	12.5	80	>100		Xe	2550	44.7	200	45
Ar	305	11.3	90	>100		Au	320	83.4	25	15
Ar	540	8	200	>100		Au	420	89.2	30	20
Kr	180	41	25	75		Au	650	93.8	40	20
Kr	230	40.8	30	75		Au	900	94.2	50	5
Kr	320	40	40	75		Au	1100	93.2	60	5
Kr	500	37.1	60	85		Au	1500	89.9	80	5
Kr	1450	23.6	200	95		Au	1700	88.1	90	5
Xe	320	67.3	30	45		Au	3750	72.6	200	5

TABLE II: A SUBSET OF THE DATA IN TABLE I

Ion	Range (μm)	Incident Energy (MeV)	Incident LET (MeV-cm^2/mg)	Vds (V)
Ar	200	540	8	>100
Kr	200	1450	23.6	95
Xe	200	2550	44.7	45
Au	200	3750	72.6	5

APPENDIX

Stopping Rates of Ions for 100 mils aluminum shielding, IGCR

						during solar minimum			during solar flare		
Atomic Number	Element	AMU	Shield Energy E (MeV)	E/m (MeV/nucleon)	LET (MeV-cm2/mg)	h* (1/m2-s-sr-MeV/nuc)	huomni (1/cm2-day-MeV)	Stopping Rate (1/cm3-day)	h* (1/m2-s-sr-MeV/nuc)	huomni (1/cm2-day-Mev)	Stopping Rate (1/cm3-day)
18	Ar	40	2860	71.59307099	2.51	3.92E-05	0.000106567	0.623233075	0.00242	0.006578853	38.47510312
36	Kr	84	8250	98.45103702	7.5	1.81E-08	2.34571E-08	0.000409913	6.00E-06	7.77584E-06	0.135882837
54	Xe	131	15700	119.579871	14.5	1.90E-09	1.5716E-09	5.30965E-05	3.89E-07	3.21764E-07	0.010870807

Stopping Rates of Ions for 250 mils aluminum shielding, IGCR

						during solar minimum			during solar flare		
Atomic Number	Element	AMU	Shield Energy E (MeV)	E/m (MeV/nucleon)	LET (MeV-cm2/mg)	h* (1/m2-s-sr-MeV/nuc)	huomni (1/cm2-day-MeV)	Stopping Rate (1/cm3-day)	h* (1/m2-s-sr-MeV/nuc)	huomni (1/cm2-day-Mev)	Stopping Rate (1/cm3-day)
18	Ar	40	4873	121.9835787	1.7	5.88E-05	0.00015985	0.633165077	2.51E-04	0.000682352	2.7027965
36	Kr	84	14320	170.8871333	5.17	1.97E-08	2.55307E-08	0.000307545	9.77E-07	1.26617E-06	0.015252365
54	Xe	131	27550	209.8360156	10.2	1.94E-09	1.60469E-09	3.8137E-05	7.34E-08	6.07134E-08	0.001442914

Fig. A: Full spreadsheet calculations of stopping rates for several examples.

TABLE A: STOPPING RATE PER UNIT VOLUME (1/cm^3-day) VERSUS ATOMIC NUMBER Z

Z	GCR 100 mils	WWF 100 mils	GCR 250 mils	WWF 250 mils	Z	GCR 100 mils	WWF 100 mils	GCR 250 mils	WWF 250 mils
1	1.74E+03	2.54E+09	1.91E+03	5.27E+08	47	2.78E-05	9.12E-04	2.00E-05	1.17E-04
2	1.58E+03	1.66E+07	9.10E+02	1.60E+06	48	7.47E-05	3.24E-03	5.37E-05	4.03E-04
3	2.14E+00	0.00E+00	2.15E+00	0.00E+00	49	1.65E-05	4.03E-04	1.19E-05	5.11E-05
4	6.50E-01	0.00E+00	8.11E-01	0.00E+00	50	8.91E-05	8.66E-03	6.42E-05	1.14E-03
5	6.84E+00	0.00E+00	7.15E+00	0.00E+00	51	1.88E-05	6.21E-04	1.36E-05	7.85E-05
6	3.93E+01	2.01E+05	3.62E+01	3.50E+03	52	1.09E-04	1.29E-02	7.87E-05	1.75E-03
7	1.17E+01	3.02E+04	9.94E+00	6.86E+02	53	2.16E-05	2.47E-03	1.55E-05	3.27E-04
8	5.79E+01	1.52E+05	4.50E+01	4.62E+03	54	5.31E-05	1.09E-02	3.81E-05	1.44E-03
9	1.05E+00	4.33E+00	9.98E-01	1.92E-01	55	1.31E-05	7.85E-04	9.34E-06	1.04E-04
10	1.04E+01	1.51E+04	8.55E+00	7.25E+02	56	1.33E-04	8.18E-04	9.59E-05	1.07E-03
11	2.31E+00	9.94E+02	1.99E+00	5.21E+01	57	1.22E-05	7.92E-04	8.64E-06	1.03E-04
12	1.49E+01	1.08E+04	1.26E+01	5.45E+02	58	3.67E-05	1.93E-03	2.61E-05	2.55E-04
13	3.04E+00	7.63E+02	2.51E+00	4.12E+01	59	8.93E-05	2.99E-04	6.36E-06	4.01E-05
14	1.16E+01	1.31E+04	9.57E+00	7.17E+02	60	3.38E-05	1.43E-03	2.38E-05	1.94E-04
15	4.00E-01	7.22E+00	3.73E-01	4.20E-01	61	4.05E-06	0.00E+00	2.85E-06	0.00E+00
16	2.03E+00	2.72E+03	1.78E+00	1.54E+02	62	3.83E-05	3.59E-04	2.71E-05	4.86E-05
17	3.25E-01	3.94E+00	3.31E-01	2.68E-01	63	6.73E-06	1.38E-04	4.73E-06	1.88E-05
18	6.23E-01	3.85E+01	6.33E-01	2.70E+00	64	2.99E-05	7.10E-04	2.12E-05	9.66E-05
19	7.41E-01	6.64E+00	6.94E-01	4.89E-01	65	7.42E-06	1.09E-04	5.29E-06	1.46E-05
20	2.86E+00	9.39E+02	2.28E+00	5.67E+01	66	3.08E-05	6.91E-04	2.17E-05	9.33E-05
21	5.18E-01	2.04E+00	4.25E-01	1.43E-01	67	1.20E-05	1.31E-04	8.40E-06	1.78E-05
22	1.92E+00	2.59E+01	1.55E+00	2.07E+00	68	1.94E-05	3.43E-04	1.37E-05	4.67E-05
23	1.17E+00	2.09E+00	8.79E-01	1.89E-01	69	4.04E-06	6.64E-05	2.84E-06	9.16E-06
24	2.30E+00	9.09E+01	1.75E+00	7.15E+00	70	1.97E-05	3.04E-04	1.40E-05	4.20E-05
25	1.49E+00	2.96E+01	1.09E+00	2.39E-05	71	2.93E-06	6.68E-05	2.06E-06	9.10E-06
26	1.25E+01	5.25E+03	9.63E+00	4.00E+02	72	1.85E-05	2.66E-04	1.30E-05	3.58E-05
27	5.38E-02	4.96E+01	4.82E-02	5.12E+00	73	1.68E-05	2.95E-05	1.18E-06	3.97E-06
28	5.99E-01	1.08E+02	4.72E-01	1.15E+01	74	1.89E-05	3.23E-04	1.32E-05	4.28E-05
29	9.05E-03	1.06E+00	6.90E-03	1.12E-01	75	6.61E-06	6.41E-05	4.63E-06	8.63E-06
30	1.19E-02	2.47E+00	9.12E-03	2.76E-01	76	2.86E-05	9.64E-04	2.00E-05	1.27E-04
31	8.87E-04	1.62E-01	6.75E-04	1.73E-02	77	1.90E-05	9.47E-04	1.33E-05	1.25E-04
32	1.98E-03	3.84E-01	1.49E-03	4.17E-02	78	3.66E-05	1.87E-03	2.55E-05	2.43E-04
33	1.27E-04	2.22E-02	9.59E-05	2.46E-03	79	6.84E-06	3.12E-04	4.78E-06	4.08E-05
34	7.54E-04	2.21E-01	5.66E-04	2.42E-02	80	1.21E-05	3.08E-04	8.41E-06	4.03E-05
35	1.44E-04	2.82E-03	1.08E-04	3.14E-03	81	3.72E-06	2.75E-04	2.60E-06	3.64E-05
36	4.10E-04	1.36E-01	3.08E-04	1.53E-02	82	3.43E-05	3.11E-03	2.39E-05	4.13E-04
37	1.36E-04	1.97E-02	1.01E-04	2.32E-03	83	1.84E-06	1.84E-04	1.28E-06	2.38E-05
38	4.57E-04	6.21E-02	3.39E-04	7.21E-03	84	0.00E+00	0.00E+00	0.00E+00	0.00E+00
39	1.05E-04	1.18E-02	7.78E-05	1.39E-03	85	0.00E+00	0.00E+00	0.00E+00	0.00E+00
40	2.64E-04	2.83E-02	1.94E-04	3.39E-03	86	0.00E+00	0.00E+00	0.00E+00	0.00E+00
41	4.90E-05	2.20E-01	3.60E-05	2.63E-04	87	0.00E+00	0.00E+00	0.00E+00	0.00E+00
42	1.41E-04	1.01E-02	1.03E-04	1.26E-03	88	0.00E+00	0.00E+00	0.00E+00	0.00E+00
43	1.66E-05	0.00E+00	1.21E-05	0.00E+00	89	0.00E+00	0.00E+00	0.00E+00	0.00E+00
44	5.49E-05	4.47E-03	4.02E-05	5.52E-04	90	2.04E-06	6.18E-05	1.41E-06	7.95E-06
45	2.89E-05	9.28E-04	2.11E-05	1.19E-04	91	0.00E+00	0.00E+00	0.00E+00	0.00E+00
46	8.34E-05	2.93E-03	6.07E-05	3.75E-04	92	1.27E-06	3.39E-05	8.76E-07	4.49E-06